Unsettling the settled: Simple musings on the complex climatic system
Supplementary Appendices SA – SD

Demetris Koutsoyiannis*, George Tsakalias

Department of Water Resources and Environmental Engineering, School of Civil Engineering, National Technical University of Athens Heroon Polytechneiou 5, 157 80 Zographou, Greece

*** Correspondence:**
Corresponding Author, dk@itia.ntua.gr

Contents

Appendix SA: On the inappropriateness of the term "greenhouse effect"

Several scholars attribute the "discovery" of the "greenhouse effect" to Arrhenius (1896) but Fleming (1998) notes that this attribution is misleading and incorrect. He adds that the history of the greenhouse effect is not well known either outside or *inside* the atmospheric sciences. What Arrhenius (1896) actually stated is: "*Fourier maintained that the atmosphere acts like the glass of a hothouse, because it lets through the light rays of the sun but retains the dark rays from the ground.*" Notably, he used the term "hothouse" instead of "greenhouse". However, as noted by Fleming (1998), Fourier's article is not in essence about the greenhouse effect.

The term "greenhouse" was likely used for first time for the atmospheric behavior by Ekholm (1901), a Swedish meteorologist who was a close colleague of Arrhenius, who wrote: "*the atmosphere may act like the glass of a green-house, letting through the light rays of the sun relatively easily, and absorbing a great part of the dark rays emitted from the ground, and it thereby may raise the mean temperature of the earth's surface*".

The first who appears to have used both terms "greenhouse effect" and "blanketing effect" for planetary atmospheres, with preference to the former, was Poynting (1907) who clearly stated, "*A planetary atmosphere no doubt acts in some such way as the greenhouse glass*." His theory was criticized a year later by Very (1908) who asserted that no reasonable modification would enable the simple formula for a glass greenhouse to fit the atmospheric conditions on our earth.

The analogy of the atmospheric behavior in terms of LW radiation, with the glass in a greenhouse or with a blanket was adopted by Humphreys (1913) who stated, "*it is true that carbon dioxide is more absorptive of terrestrial than of solar radiation, and that it therefore produces a green-house or blanketing effect*". Likewise, Trewartha (1954; first edition in 1937) wrote: "*The greenhouse depends* *for a large part of it heating upon the principle that the glass roof and sides permit free entrance of solar energy but, on the other hand, prevent the escape of long-wave heat energy.*"

The analogy had earlier been refuted by Wood (1909) based on an experiment using two similar boxes, but one having a glass cover and the other a cover of rock salt. He observed a maximum temperature of about 55 °C in each box when exposed to the sun and concluded that the function of the cover is mainly to prevent the loss of heat by convection (air flow), rather than the escape of LW radiation. Based on this finding he stated, "*It seems to me very doubtful if the atmosphere is warmed to any great extent by absorbing the radiation from the ground.*" Abbot (1909) discussed Wood's (1909) work and agreed thar the main function of the cover of a "hot-box" or "hot-house" is to prevent loss of heat by convection. On the other hand, he opined that in the atmosphere there was a "blanket effect" that results in a temperature increase of 31 °C.

Several modern scholars have repeated Wood's (1909) experiment or different settings thereof (Nahle, 2011a,b; Spencer, 2013a,b; Pratt, 2016; Seim and Olsen, 2020; Arveson, 2023) finding contradicting results. However, even the supporters of the GHE concept in fact verify with their experiments the dominance of preventing loss of heat by convection, rather than GHE. For example, Arveson (2023; his Fig. 5) found that in his experimental hotbox covered by polyethylene, which does not prevent the escape of LW radiation, the temperature increased from ambient temperatures 5-25 °C to more than 90 °C. At the same time, in his glass-covered hotbox the typical difference in temperature was 8 °C. In other words, preventing heat loss by convection has an effect of about an order of magnitude higher than preventing heat loss by LW radiation. This is confirmed by the fact that in several countries (e.g. Greece) real-world greenhouses are typically covered by polyethylene films rather than glass.

The most sophisticated and informative experiments on atmospheric behavior are those of Harde and Schnell (2022) and Schnell and Harde (2023). Their measurements are also confirmed by radiative transfer calculations. Their results suggest that ARE contributes to some warming of the Earth's surface, but not to any remarkable direct warming of the air temperature (see also Section 3.4).

It is noted that the Intergovernmental Panel on Climate Change (IPCC), does not make any cautionary note about the inappropriateness of the term GHE, which it uses massively in all its assessment reports, from the first (IPCC, 1990) to the last (IPCC, 2021). In particular, in its fourth assessment report (IPCC, 2007) it uses equivalently the term blanketing effect: "*The reason the Earth's surface is this warm is the presence of greenhouse gases, which act as a partial blanket for the longwave radiation coming from the surface.* […] *Clouds, on the other hand, do exert a blanketing effect similar to that of the greenhouse gases; however, this effect is offset by their reflectivity, such that on average, clouds tend to have a cooling effect on climate (although locally one can feel the warming effect: cloudy nights tend to remain warmer than clear nights because the clouds radiate longwave energy back down to the surface).*"

Similar is the situation in glossaries of several learned societies, such as WMO (1992) which severely misrepresents the term "greenhouse climate/climat de serre". The United States National Oceanography and Atmospheric Administration (NOAA) does not issue any warning in its glossaries (NOAA, undated 1,2) but it does so in other information sites. Thus, NOAA (undated 3) states: "*This atmospheric process is referred to as the Greenhouse Effect, since both the atmosphere and a greenhouse act in a manner which retains energy as heat. However, this is an imperfect analogy. A greenhouse works primarily by preventing warm air (warmed by incoming solar radiation) close to the ground from rising due to convection, whereas the atmospheric Greenhouse Effect works by preventing infrared radiation loss to space.*" The American Chemical Society (ACS, undated) used to promote the following clear warning, which looks to have been withdrawn after 2024: "*The atmospheric gases and a greenhouse work in quite different ways, but the resulting effect, higher temperature in both cases, has led to the nomenclature 'greenhouse gases' for the atmospheric gases responsible for the atmospheric warming effect. Although this nomenclature is misleading, it is in such common use that we use it here as well.*" Also the American Institute of Physics (AIP, 2025) clarifies that "*greenhouses are kept warm less by the radiation properties of glass than because the heated air cannot rise and blow away*". Additional information on the subject can be found in Gerlich and Tscheuschner (2009) and Arveson (2023).

Based on the above review of experiments and related documents, we may summarize the flaws of the "greenhouse effect" analogy in the following points.

Mechanism mismatch: convection vs. radiation and implication of a static barrier

In a real greenhouse, heat is trapped primarily by preventing convection—the glass or plastic cover stop warm air from escaping, keeping the interior warm. In contrast, ARE relies on radiative processes, where RAGs absorb and re-emit radiation. A greenhouse has fixed glass or plastic cover and walls that create a controlled, enclosed environment. The atmosphere, however, is dynamic, with gases mixing, circulating, and interacting across layers.

The analogy would suggest that physical barriers are involved, which does not accurately reflect the molecular-level radiative absorption in the atmosphere. Furthermore, the analogy would imply a static, uniform heat trap, whereas ARE varies by location, altitude, and time due to atmospheric dynamics. Adopting the analogy would mislead people into thinking the atmosphere is a sealed system, protected by a blanket, and ignoring its fluid and variable nature.

Oversimplification and non-holistic view of complex processes

Radiation in the atmosphere involves multiple factors, various RAGs with their specific absorption spectra, altitude and lapse rate effects, interaction of atmosphere with land and oceans, and feedback loops. The greenhouse analogy reduces them all to a single image of heat being trapped, like in a glass structure. It glosses over critical details, such as how different processes contribute to temperature changes or how heat is redistributed globally. The analogy leads to misconceptions about the scale and nature of atmospheric processes, making it harder to grasp the accurate scientific picture.

An idea of the oversimplification and non-holistic view of the complex processes is provided by Figure SA1. It can readily be seen in Figure SA1 that the most important RAG, WV, and even the CO_2, are radiatively active not only in LW but also in SW radiation. Furthermore, as seen in Figure SA2 (left), constructed by RRTM, the SW radiation is not a universal constant but varies with altitude, and the variation becomes substantial in the presence of RAGs. Furthermore, as seen in Figure SA2 (right), the LW downward radiation flux is strongly correlated with the SW downward radiation flux in a negative pattern. Isolating the LW radiation, as the greenhouse analogy implies, is totally unscientific.

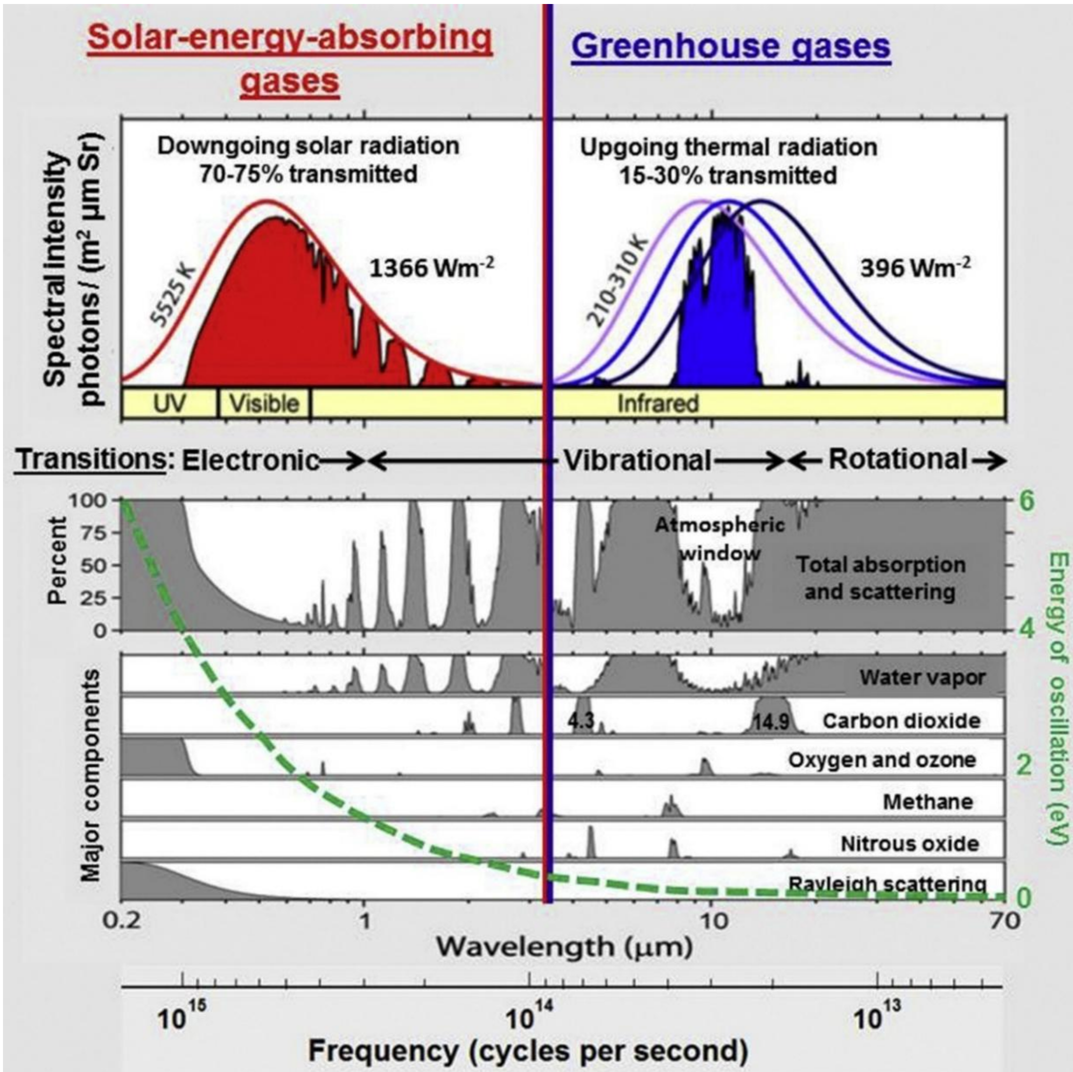

Figure SA1 Transmission of SW (solar) and LW (Earth's) radiation through atmosphere, vs. wavelength and frequency. For comparison with Figure 1, the wavenumbers of 400 and 1600 cm^{-1} correspond to wavelengths of 25 and 6.25 µm, respectively. Reproduced from Wei et al. (2019; their Figure 1 under the CC BY license.)

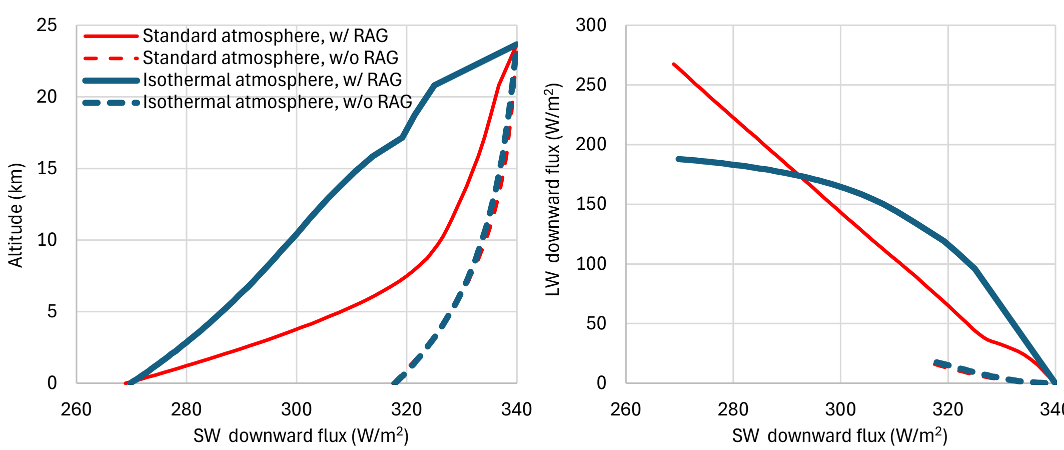

Figure SA2 (left) SW downward energy flux as a function of altitude for the indicated cases, standard or isothermal atmosphere, with or without RAGs, and without clouds; (**right**). LW downward energy flux as a function of SW downward energy flux for the same cases. The default values are used for all other RRTM parameters.

Unjustified emphasis on RAGs

As shown in Sections 3.4 – 3.6, it is the temperature gradient that makes the surface-level temperature increase from about 252 K to about 288 K (i.e. by 36 K), with RAGs playing a secondary role. The temperature increase does not reflect a "greenhouse effect", but it is mainly the result of the temperature gradient, whose origin is not the ARE but the processes described in section 3.5.

On the other hand, a real greenhouse maintains a relatively uniform warm temperature inside. Thus, the analogy implies that the entire atmosphere warms uniformly, missing climate dynamics. In the atmosphere, the ARE warms the surface and the lower atmosphere but not the upper troposphere, while it may cool the stratosphere due to radiative dynamics.

Additional problems

The greenhouse analogy treats all RAGs as a monolithic glass barrier rather than a diverse set of molecules, each one with unique properties. The analogy promotes the idea of a heat trap, leading to misrepresentation of how the Earth's energy balance works. Unlike the heat blocking from the glass, the atmosphere does not fully block infrared radiation, with some escaping to space and some being re-emitted back to Earth's surface.

Appendix SB: Maximum entropy of a single monoatomic molecule

We consider an air column with a square cross section of edge a containing monoatomic molecules of mass m_0, assumed to be spherical particles, in fast motion. We do not know their exact position and velocity (actually, it is infeasible to know them). We wish to find the marginal probability distribution of one of these particles. Its state is described by 6 variables, 3 indicating its position $\underline{x}_i$ and 3 indicating its velocity $\underline{u}_i$ with $i = 1,2,3$, all represented as stochastic variables, forming the vector $\underline{\boldsymbol{z}} \coloneqq (\underline{x}_1, \underline{x}_2, \underline{x}_3, \underline{u}_1, \underline{u}_2, \underline{u}_3)$. Notice that here we use the Dutch convention to underline stochastic (random) variables, while their values are not underlined. We denote $f(\boldsymbol{z})$ the probability density function. The constraints for the particle's position are:

$$0 \le \underline{x}_{1,2} \le a, \qquad \underline{x}_3 \ge 0 \tag{SB1}$$

We use a non-relativistic framework and therefore we do not constrain velocity. The feasible space, Ω, is thus $\Omega \coloneqq \{0 \le x_{1,2} \le a, x_3 \ge 0, -\infty < u_i < \infty; i = 1,2,3\}$.

As the column is not in motion, conservation of momentum demands that $\mathrm{E}[m_0 \underline{u}_i] = m_0 \int_\Omega u_i f(\boldsymbol{z}) \mathrm{d}\boldsymbol{z} = 0$, or:

$$\mathrm{E}[\underline{u}_i] = 0, \qquad i = 1,2,3 \tag{SB2}$$

We note that, in general, the expectation $\mathrm{E}[\underline{u}_i]$ represents macroscopic motion, while $u_i - \mathrm{E}[\underline{u}_i]$ represents fluctuation at a microscopic level. (In our case the fluctuation is identical to u_i.)

The conservation of energy demands that the sum of *internal* (or *thermal*) *energy* and the dynamic energy of the particle be constant, equal to the energy per particle, ε. The former is $\mathrm{E}\left[m_0 \|\underline{u}\|^2/2\right] =$

$(m_0/2)\int_\Omega \|\underline{u}\|^2 f(\boldsymbol{z})\mathrm{d}\boldsymbol{z}$, where $\|\underline{u}\|^2 = \underline{u}_1^2 + \underline{u}_2^2 + \underline{u}_3^2$, and the latter is $m_0 g \underline{x}_3$, where g is the gravity acceleration. Hence, the energy constraint is

$$\mathrm{E}\left[\|\underline{u}\|^2 + 2g\underline{x}_3\right] = \frac{2\varepsilon}{m_0} \tag{SB3}$$

Now we form the entropy of $\underline{\boldsymbol{z}}$ according to the entropy definition:

$$\Phi[\underline{\boldsymbol{z}}] := \mathrm{E}\left[-\ln\frac{f(\underline{\boldsymbol{z}})}{\beta(\underline{\boldsymbol{z}})}\right] = -\int_\Omega \ln\frac{f(\boldsymbol{z})}{\beta(\boldsymbol{z})} f(\boldsymbol{z})\mathrm{d}\boldsymbol{z} \tag{SB4}$$

where $\beta(\boldsymbol{z})$ is a background density, assumed to be of Lebesgue form. We recognize from the quantity $\ln(f(\boldsymbol{z})/\beta(\boldsymbol{z}))$ that the latter should have units $[z^{-1}] = [x^{-3}]\,[u^{-3}] = [\mathrm{L}^{-6}\,\mathrm{T}^3]$. To form this, we utilize a universal constant, i.e., the Planck constant $h = 6.626 \times 10^{-34}$ J s; its dimensions are $[\mathrm{L}^2\,\mathrm{M}\,\mathrm{T}^{-1}]$. If we combine it with the particle mass m_0, we observe that the quantity $(m_0/h)^3$ has the required dimensions $[\mathrm{L}^{-6}\,\mathrm{T}^3]$, thereby giving the entropy as

$$\Phi[\underline{\boldsymbol{z}}] := \mathrm{E}\left[-\ln\left(\left(\frac{h}{m_0}\right)^3 f(\underline{\boldsymbol{z}})\right)\right] = -\int_\Omega \ln\left(\left(\frac{h}{m_0}\right)^3 f(\boldsymbol{z})\right) f(\boldsymbol{z})\mathrm{d}\boldsymbol{z} \tag{SB5}$$

Notice that here we have not multiplied the entropy with the Boltzmann constant $k = 1.381\times10^{-23}$ J K^{-1} and that $\Phi[\underline{\boldsymbol{z}}]$ is dimensionless.

To apply the principle of maximum entropy with constraints in Equations (SB1) – (SB3), plus the unity integral of the density function, we form the Lagrangian (using Lagrange multipliers $l_i, i = 0, \ldots, 4$):

$$\begin{aligned} A := &-\int_\Omega \ln\left(\left(\frac{h}{m_0}\right)^3 f(\boldsymbol{z})\right) f(\boldsymbol{z})\mathrm{d}\boldsymbol{z} - l_0\left(\int_\Omega f(\boldsymbol{z})\mathrm{d}\boldsymbol{z} - 1\right) - \sum_{i=1}^{3} l_i \int_\Omega u_i f(\boldsymbol{z})\mathrm{d}\boldsymbol{z} \\ &- l_4\left(\int_\Omega \left(u_1^2 + u_2^2 + u_3^2 + 2g\underline{x}_3\right) f(\boldsymbol{z})\mathrm{d}\boldsymbol{z} - \frac{2\varepsilon}{m_0}\right) \end{aligned} \tag{SB6}$$

Taking the functional derivative, we find

$$\frac{\partial A}{\partial f(\boldsymbol{z})} = -\ln\left(\left(\frac{h}{m_0}\right)^3 f(\boldsymbol{z})\right) - 1 - l_0 - \sum_{i=1}^{3} l_i\, u_i - l_4\left(u_1^2 + u_2^2 + u_3^2 + 2g\underline{x}_3\right) = 0 \tag{SB7}$$

After algebraic manipulations, we eventually find the distribution of $\underline{\boldsymbol{z}}$ as:

$$f(\boldsymbol{z}) = \frac{2}{\pi^{3/2}}\left(\frac{1}{a}\right)^2 \left(\frac{5m_0}{4\varepsilon}\right)^{5/2} g \exp\left(-\frac{5m_0}{4\varepsilon}\left(\|\underline{u}\|^2 + 2gx_3\right)\right) \tag{SB8}$$

Indeed, $f(\boldsymbol{z})$ in Equation (SB8) satisfies all constraints, as it is trivial to show that:

$$\int_\Omega f(\boldsymbol{z})\,\mathrm{d}\boldsymbol{z} = 1, \qquad \int_\Omega u_i f(\boldsymbol{z})\,\mathrm{d}\boldsymbol{z} = 0, \qquad \int_\Omega (u_1^2 + u_2^2 + u_3^2 + 2gx_3)\, f(\boldsymbol{z})\mathrm{d}\boldsymbol{z} = \frac{2\varepsilon}{m_0} \tag{SB9}$$

To find the marginal distribution of each of the variables we integrate over the domain of the remaining variables. Thus, the marginal distribution of each of the location coordinates $\underline{x_i}$ is easily found to be,

$$f_{x_1}(x_1) = f_{x_2}(x_2) = \frac{1}{a}, \qquad 0 \le x_1, x_2 \le a, \qquad f_{x_3}(x_3) = \frac{5gm_0}{2\varepsilon}\exp\left(-\frac{5gm_0}{2\varepsilon}x_3\right) \tag{SB10}$$

As $f_{x_3}(x_3)$ is proportional to air density, the last equation shows that the density decreases exponentially with altitude. The marginal distribution of each of the velocity coordinates $\underline{u_i}$ is derived from Equation (SB8) as

$$f_{u_i}(u_i) = \left(\frac{5m_0}{4\pi\varepsilon}\right)^{1/2} \exp\left(-\frac{5m_0}{4\varepsilon}u_i^2\right) \tag{SB11}$$

This is Gaussian with mean 0 and variance $2\varepsilon/5m_0$.

Furthermore, we readily deduce from the above results that the joint distribution $f(\boldsymbol{z})$ is a product of functions of $\boldsymbol{z}$'s coordinates $(x_1, x_2, x_3, u_1, u_2, u_3)$. This means that all six stochastic variables are jointly independent. The independence results from entropy maximization. From Equations (SB8) and (SB11) we also observe a symmetry with respect to the three velocity coordinates, resulting in equipartition of the total energy ε into $\varepsilon/5$ for each direction or degree of freedom. This is known as the *equipartition* principle and is again a result of entropy maximization. In other words, neither independence nor equipartition are posed as assumptions here. Clearly, they are derived by the principle of maximum entropy (that is, maximum uncertainty).

To find the marginal distribution of the velocity magnitude $\|\underline{u}\|$, we recall that the sum of squares of n independent $N(0,1)$ stochastic variables has a $\chi^2(n)$ distribution (Papoulis, 1990, pp. 219, 221) and then we use known results for the density of a transformation of a stochastic variable (Papoulis, 1990, p. 118) to obtain the distribution of the square root. The result is the Maxwell–Boltzmann distribution:

$$f_{\|\underline{u}\|}(\|\underline{u}\|) = \frac{4}{\sqrt{\pi}}\left(\frac{5m_0}{4\varepsilon}\right)^{3/2} \|\underline{u}\|^2 \exp\left(-\frac{5m_0}{4\varepsilon}\|\underline{u}\|^2\right) \tag{SB12}$$

Once $f(\boldsymbol{z})$ has been determined in Equation (SB8), the mean energy can be partitioned into thermal and dynamic (due to gravity) as follows:

$$\varepsilon_\theta := \mathrm{E}\left[m_0\|\underline{u}\|^2/2\right] = \frac{3\varepsilon}{5}, \qquad \varepsilon_g := \mathrm{E}\left[m_0 g \underline{x}_3\right] = \frac{2\varepsilon}{5} \tag{SB13}$$

Given that the kinetic state of a monoatomic molecule has three degrees of freedom (one per direction of motion), the above result shows that gravity is equivalent to two additional degrees of freedom.

The final expression of entropy is then obtained as follows. We observe that

$$-\ln f(\boldsymbol{z}) = 2\ln a + \frac{5}{2}\ln\left(\frac{4\pi\varepsilon}{5m_0}\right) - \ln(2\pi g) + \frac{5m_0}{4\varepsilon}\left(u_1^2 + u_2^2 + u_3^2 + 2gx_3\right),$$
$$\ln\beta(\boldsymbol{z}) = 3\ln\frac{m_0}{h} \tag{SB14}$$

After performing the integration over Ω we find

$$\Phi[\underline{\boldsymbol{z}}] = \frac{5}{2}\ln\left(\frac{2^{8/5}\pi^{3/5}\mathrm{e}}{5}\,\frac{m_0^{1/5}}{g^{2/5}h^{6/5}}\,\varepsilon a^{4/5}\right) \tag{SB15}$$

where e is the base of natural logarithms. It can be verified that the equation is dimensionally consistent and that $\Phi[\underline{\boldsymbol{z}}]$ is dimensionless as it should be.

The temperature is defined as the inverse of the partial derivative of entropy with respect to thermal energy, i.e.,

$$\frac{1}{\theta} := \left(\frac{\partial\Phi}{\partial\varepsilon_\theta}\right)_{V,N} \tag{SB16}$$

where the meaning of the subscripts is that the volume V and number of particles N should be constant. Notice that in this definition, temperature has units of energy and to convert it to the thermodynamic temperature T we must divide it by Boltzmann constant ($T = \theta/k$). In our case $N = 1$ and the V of the column is infinite, and thus we replace it with the mean of the volume, regarded as a stochastic variable, i.e.

$$\mu_V := \mathrm{E}[\underline{V}] = a^2\mathrm{E}[\underline{x}_3] = a^2\int_0^\infty \frac{5gm_0}{2\varepsilon}\exp\left(-\frac{5gm_0}{2\varepsilon}x_3\right)\mathrm{d}x_3 = \frac{2\varepsilon a^2}{5gm_0} \tag{SB17}$$

so that, to have constant μ_V the size a should be

$$a = \left(\frac{5gm_0}{2\varepsilon}\mu_V\right)^{1/2} \tag{SB18}$$

Equation (SB15) can then be written as

$$\Phi[\underline{z}] = \frac{5}{2}\ln\left(\frac{2^{6/5}\pi^{3/5}\mathrm{e}}{3^{3/5}}\,\frac{m_0^{3/5}}{h^{6/5}}\,\varepsilon_\theta^{3/5}\mu_V^{2/5}\right) \tag{SB19}$$

Taking the derivative with respect to ε_θ, we easily find

$$\frac{1}{\theta} = \frac{\partial\Phi}{\partial\varepsilon_\theta} = \frac{3}{2\varepsilon_\theta} \Rightarrow \theta = \frac{2\varepsilon_\theta}{3} \tag{SB20}$$

The above analysis was made for the entire air column. Next, we will fix the altitude to a specific value x_3 and find the same quantities conditional on this altitude. Using the subscript C for conditional, in this case we have

$$f_\mathrm{C}(\boldsymbol{z}|x_3) = \frac{f(\boldsymbol{z})}{f_{x_3}(x_3)} = \left(\frac{1}{a}\right)^2 \left(\frac{5m_0}{4\pi\varepsilon}\right)^{3/2} \exp\left(-\frac{5m_0}{4\varepsilon}\left(\|\underline{u}\|^2\right)\right) \tag{SB21}$$

where we observe that the conditional probability density does not depend on the altitude x_3. Now the integration volume is $\Omega_\mathrm{C} \coloneqq \{0 \le x_{1,2} \le a, -\infty < u_i < \infty; i = 1,2,3\}$. Integrated over this volume, the mean energy is:

$$\varepsilon_\theta = \mathrm{E}\left[m_0\|\underline{u}\|^2/2\right] = \int_{\Omega_\mathrm{C}} (u_1^2 + u_2^2 + u_3^2)\, f_\mathrm{C}(\boldsymbol{z})\mathrm{d}\boldsymbol{z} = \frac{3\varepsilon}{5} \tag{SB22}$$

This is the same as in the unconditional case. The potential energy is fixed, $\varepsilon_g = m_0 g x_3$, and its average over the column is

$$\varepsilon_g \coloneqq \int_0^\infty m_0 g x_3 f_{x_3}(x_3)\mathrm{d}x_3 = \frac{2\varepsilon}{5} \tag{SB23}$$

which agrees with the previous result.

The entropy is not easy to calculate in conditional mode, as an assumption is needed for adapting the background measure $\beta(\boldsymbol{z})$. For this reason, we follow a different approach, replacing the condition $\underline{x}_3 = x_3$ with $x_3 - a/2 \le \underline{x}_3 \le x_3 + a/2$, so that no change to the background measure be necessary. In order for this approximation to be valid, we assume $a \ll x_3$, which is not a problem as we can make a as small as we wish. In this case, a uniform distribution for the location of the molecule in the cube is plausible. Based on the results in Koutsoyiannis (2014) and substituting $3\varepsilon/5$ for ε, we have

$$f_\mathrm{F}(\boldsymbol{z}) = \left(\frac{1}{a}\right)^3 \left(\frac{5m_0}{4\pi\varepsilon}\right)^{3/2} \exp\left(-\frac{5m_0}{4\varepsilon}\left(\|\underline{u}\|^2\right)\right) \tag{SB24}$$

where the subscript F stands for "fixed x_3" and the only difference from Equation (SB21) is that a is cubed, rather than squared. The thermal energy is then found to be

$$\varepsilon_\theta = \frac{3\varepsilon}{5} \tag{SB25}$$

i.e., the same as above. The entropy is

$$\Phi_{\mathrm{F}}[\underline{z}] = \frac{3}{2} \ln\left(\frac{4\pi\mathrm{e}}{5} \frac{m_0}{h^2} \varepsilon a^2\right) \tag{SB26}$$

and the temperature

$$\frac{1}{\theta_{\mathrm{F}}} = \frac{\partial \Phi_{\mathrm{F}}}{\partial \varepsilon} / \frac{\partial \varepsilon_\theta}{\partial \varepsilon} = \frac{3}{2\varepsilon} / \frac{3}{5} \Rightarrow \theta_F = \frac{2\varepsilon}{5} = \frac{2\varepsilon_\theta}{3} \tag{SB27}$$

which is constant, independent of x_3.

Appendix SC: Maximum entropy of a single diatomic molecule

In diatomic gases, which constitute the vast majority in the atmosphere (N_2, O_2), in addition to the kinetic energy, we have rotational energy at two axes x_4 and x_5 perpendicular to the axis defined by the two molecules. These energies are $L_4^2/2I$ and $L_5^2/2I$, where L denotes angular momentum at the two axes x_4 and x_5 (dimensions [M L^2 T^{-1}]) and I denotes rotational inertia (dimensions [M L^2]). Due to symmetry, $I_4 = I_5 = I$.

We consider again the same column with square cross section of edge a, containing identical diatomic molecules, each one with mass m_0, rotational inertia I, and sum of kinetic, rotational and dynamic energy ε. Each molecule is described by eight variables, three indicating its position, $\underline{x}_i$, three indicating its velocity $\underline{u}_i$ ($i = 1,2,3$) and two indicating its rotation, $\underline{u}_4 = \underline{L}_4/\sqrt{I m_0}$ and $\underline{u}_5 = \underline{L}_5/\sqrt{I m_0}$. Note that the coordinates $\underline{u}_4$ and $\underline{u}_5$ were chosen so as have the same dimensions as all other $\underline{u}_i$ and $m_0 u_i^2/2, i = 4,5$ represent the rotational energy. The coordinates $\underline{x}_1, \underline{x}_2, \underline{x}_3$ and the five $\underline{u}_i$ are represented as stochastic variables, forming the vector $\underline{\boldsymbol{z}} = (\underline{x}_1, \underline{x}_2, \underline{x}_3, \underline{u}_1, \underline{u}_2, \underline{u}_3, \underline{u}_4, \underline{u}_5)$.

The constraints are the same as in Appendix SB (Equations (SB1) – (SB3)). The background density $\beta(x)$ in $\ln(f(x)/\beta(x))$ should have units $[z^{-1}] = [x^{-3}]\,[u^{-5}] = [L^{-8}\,T^5]$. Combining the Planck constant h with the particle mass m_0 and rotational inertia I, we observe that the required dimensions are attained by the quantity $m_0^4 I/h^5$, thereby giving the entropy as

$$\Phi[\underline{z}] \coloneqq \mathrm{E}\left[-\ln\left(\frac{h^5}{m_0^4 I} f(\underline{z})\right)\right] = -\int_\Omega \ln\left(\frac{h^5}{m_0^4 I} f(\boldsymbol{z})\right) f(\boldsymbol{z}) \mathrm{d}\boldsymbol{z} \tag{SC1}$$

Application of the principle of maximum entropy with constraints in Equations (SB1) – (SB3) plus the unity integral of the density function will give the density of $\underline{\boldsymbol{z}}$ as:

$$f(\boldsymbol{z}) = \frac{2}{\pi^{5/2}} \left(\frac{1}{a}\right)^2 \left(\frac{7m_0}{4\varepsilon}\right)^{7/2} g \exp\left(-\frac{7m_0}{4\varepsilon}\left(\|\underline{u}\|^2 + 2gx_3\right)\right) \tag{SC2}$$

which is again uniform for the location coordinates x_1, x_2, exponential for the location coordinate x_3, and Gaussian for the translational and rotation coordinates. The entropy is then calculated as

$$\Phi[\underline{z}] = \frac{7}{2}\ln\left(\frac{2^{12/7}\pi^{5/7}\mathrm{e}}{7}\frac{m_0^{1/7} I^{2/7}}{g^{2/7}h^{10/7}}\varepsilon a^{4/7}\right) \tag{SC3}$$

The marginal distribution of each of the location coordinates $\underline{x}_i$ is easily found to be

$$f_{x_1}(x_1) = f_{x_2}(x_2) = \frac{1}{a}, \qquad 0 \le x_1, x_2 \le a, \qquad f_{x_3}(x_3) = \frac{7gm_0}{2\varepsilon}\exp\left(-\frac{7gm_0}{2\varepsilon}x_3\right) \tag{SC4}$$

Again, the last equation shows that the density decreases exponentially with altitude. The marginal distribution of each of the velocity coordinates $\underline{u}_i$ is derived as

$$f_{u_i}(u_i) = \left(\frac{7m_0}{4\pi\varepsilon}\right)^{1/2} \exp\left(-\frac{7m_0}{4\varepsilon}u_i^2\right) \tag{SC5}$$

This is Gaussian with mean 0 and variance $2\varepsilon/7m_0$.

Once $f(\boldsymbol{z})$ has been determined in Equation (SC2), the mean energy can be partitioned into thermal and dynamic (due to gravity) as follows:

$$\varepsilon_\theta \coloneqq \mathrm{E}\left[m_0\|\underline{u}\|^2/2\right] = \frac{5\varepsilon}{7}, \qquad \varepsilon_g \coloneqq \mathrm{E}[m_0 g \underline{x}_3] = \frac{2\varepsilon}{7} \tag{SC6}$$

Given that the kinetic state of a diatomic molecule has five degrees of freedom, the above result shows that gravity is equivalent to two additional degrees of freedom. Furthermore, we readily deduce from the above results that the joint distribution $f(\boldsymbol{z})$ is a product of functions of $\boldsymbol{z}$'s coordinates $(x_1, x_2, x_3, u_1, u_2, u_3, u_4, u_5)$. This means that all eight stochastic variables are jointly independent. The independence results from entropy maximization. From Equations (SC2) and (SC5) we also observe a symmetry with respect to the five kinetic coordinates, resulting in equipartition of the total energy ε into $\varepsilon/7$ for each degree of freedom (*equipartition* principle, a result of entropy maximization).

The mean volume of the column, regarded as a stochastic variable, is

$$\mu_V \coloneqq \mathrm{E}[\underline{V}] = a^2\mathrm{E}[\underline{x}_3] = a^2 \int_0^\infty \frac{7gm_0}{2\varepsilon}\exp\left(-\frac{7gm_0}{2\varepsilon}x_3\right)\mathrm{d}x_3 = \frac{2\varepsilon a^2}{7gm_0} \tag{SC7}$$

so that, to have constant μ_V the size a should be

$$a = \left(\frac{7gm_0}{2\varepsilon}\mu_V\right)^{1/2} \quad \text{(SC8)}$$

Equation (SC3) can then be written as

$$\Phi[\underline{\boldsymbol{z}}] = \frac{7}{2}\ln\left(\frac{2^{12/7}\pi^{5/7}\mathrm{e}}{5^{5/7}2^{2/7}}\,\frac{m_0^{3/7}I^{2/7}}{h^{10/7}}\,\varepsilon_\theta^{5/7}\mu_V^{2/7}\right) \quad \text{(SC9)}$$

Taking the derivative with respect to ε_θ, we easily find

$$\frac{1}{\theta} = \frac{\partial\Phi}{\partial\varepsilon_\theta} = \frac{5}{2\varepsilon_\theta} \Rightarrow \theta = \frac{2\varepsilon_\theta}{5} \quad \text{(SC10)}$$

This has units of energy and to convert it to the thermodynamic temperature T we must divide it by Boltzmann constant ($T = \theta/k$).

The above analysis was made for the entire air column. Next, we will fix the altitude to a specific value x_3 and find the same quantities conditional on this altitude. Using the subscript C for conditional, in this case we have

$$f_\mathrm{C}(\boldsymbol{z}|x_3) = \frac{f(\boldsymbol{z})}{f_{x_3}(x_3)} = \left(\frac{1}{a}\right)^2\left(\frac{7m_0}{4\pi\varepsilon}\right)^{5/2}\exp\left(-\frac{7m_0}{4\varepsilon}\left(\|\underline{u}\|^2\right)\right) \quad \text{(SC11)}$$

where we observe that the conditional probability density does not depend on the altitude x_3. Now the integration volume is $\Omega_\mathrm{C} \coloneqq \{0 \le x_{1,2} \le a, -\infty < u_i < \infty; i = 1, \dots, 5\}$. Integrated over this volume, the mean energy is:

$$\varepsilon_\theta = \mathrm{E}\left[m_0\|\underline{u}\|^2/2\right] = \int_{\Omega_\mathrm{C}}(u_1^2 + u_2^2 + u_3^2 + u_4^2 + u_5^2)\, f_\mathrm{C}(\boldsymbol{z})\mathrm{d}\boldsymbol{z} = \frac{5\varepsilon}{7} \quad \text{(SC12)}$$

This is the same as in the unconditional case. The potential energy is fixed, $\varepsilon_g = m_0 g x_3$, and its average over the column is

$$\varepsilon_g \coloneqq \int_0^\infty m_0 g x_3 f_{x_3}(x_3)\mathrm{d}x_3 = \frac{2\varepsilon}{7} \quad \text{(SC13)}$$

in consistence with the previous result.

To calculate entropy in conditional mode, we again assume a fixed cube with edge a centered at the altitude x_3, with $a \ll x_3$, so that a uniform distribution for the location of the molecule in the cube be plausible. In this case, based on the results in Koutsoyiannis (2014) and substituting $5\varepsilon/7$ for ε, we have

$$f_{\mathrm{F}}(\boldsymbol{z}) = \left(\frac{1}{a}\right)^3 \left(\frac{7m_0}{4\pi\varepsilon}\right)^{5/2} \exp\left(-\frac{7m_0}{4\varepsilon}\left(\|\underline{u}\|^2\right)\right) \tag{SC14}$$

with the same thermal energy

$$\varepsilon_\theta = \frac{5\varepsilon}{7} \tag{SC15}$$

entropy,

$$\Phi_{\mathrm{F}}[\underline{\boldsymbol{z}}] = \frac{5}{2}\ln\left(\frac{4\pi\mathrm{e}}{7}\,\frac{m_0^{3/5} I^{2/5}}{h^2}\,\varepsilon a^{6/5}\right) \tag{SC16}$$

and temperature

$$\frac{1}{\theta_{\mathrm{F}}} = \frac{\partial \Phi_{\mathrm{F}}}{\partial \varepsilon} / \frac{\partial \varepsilon_\theta}{\partial \varepsilon} = \frac{5}{2\varepsilon} / \frac{5}{7} \Rightarrow \theta_F = \frac{2\varepsilon}{7} = \frac{2\varepsilon_\theta}{5} \tag{SC17}$$

which is constant, independent of x_3.

Appendix SD: Molecular motion simulation

Simulation setup

We conducted a molecular dynamics simulation to validate the theoretical expectation that, in the absence of convection and radiation, the atmosphere should be isothermal. The simulation software was developed in-house and is available for testing within the Supplementary Information of the paper and at https://www.itia.ntua.gr/2537/. The software architecture follows the principles of event-driven simulations, as described by Pöschel and Schwager (2005).

The system consists of 100 000 particles with a kinetic diameter of 3.64×10^{-10} m and molecular mass of 4.65×10^{-26} kg—parameters closely resembling those of nitrogen molecules. We assume the particles behave as perfectly elastic hard spheres. The simulation box has a size of L = 1.55×10^{-7} m. A gravitational field of –9.8 m/s^2 is applied vertically along the vertical axis ($z \equiv x_3$).

The simulation uses periodic boundary conditions along the horizontal axes ($x \equiv x_1, y \equiv x_2$) and reflective boundaries in the plane perpendicular to the *z*-axis. When a molecule hits the bottom boundary, its vertical velocity component u_z is reversed, while u_x and u_y remain unchanged.

The total initial energy was chosen such that particles rarely reach the top boundary, as seen in the accompanying videos (available within the Supplementary Information of the paper and at https://www.itia.ntua.gr/2537/). Additionally, as seen in Figure SD2 (right), the density at the top 1% part of the simulation box is just 0.00004% of that at the bottom 1% part. Thus, the setup effectively simulates an infinite column with reflective surface, with gas confinement due solely to gravity.

Energy and momentum are conserved in the system. More specifically, the system's total energy (kinetic plus potential) is precisely conserved, while, due to the reflections at the bottom boundary, the total momentum fluctuates, yet it is conserved statistically.

As can be seen in the videos, initially the particles are uniformly distributed up to about 30% of the box height, with small random deviations in x and y directions. We then allow the system to evolve under gravity until it reaches a stationary dynamic state. The simulation runs for 1.2 billion collisions, averaging 24 000 collisions per particle.

Velocity distribution

We periodically sampled velocities along the three axes. As shown in Figure SD1, the velocity distribution along the x axis closely matches a normal distribution with the same mean and variance. An Anderson-Darling (AD) test for normality yielded a statistic of 0.31, indicating that we cannot reject a normality hypothesis (like in the classical 1D Maxwell-Boltzmann form). Same findings hold for the y and z direction.

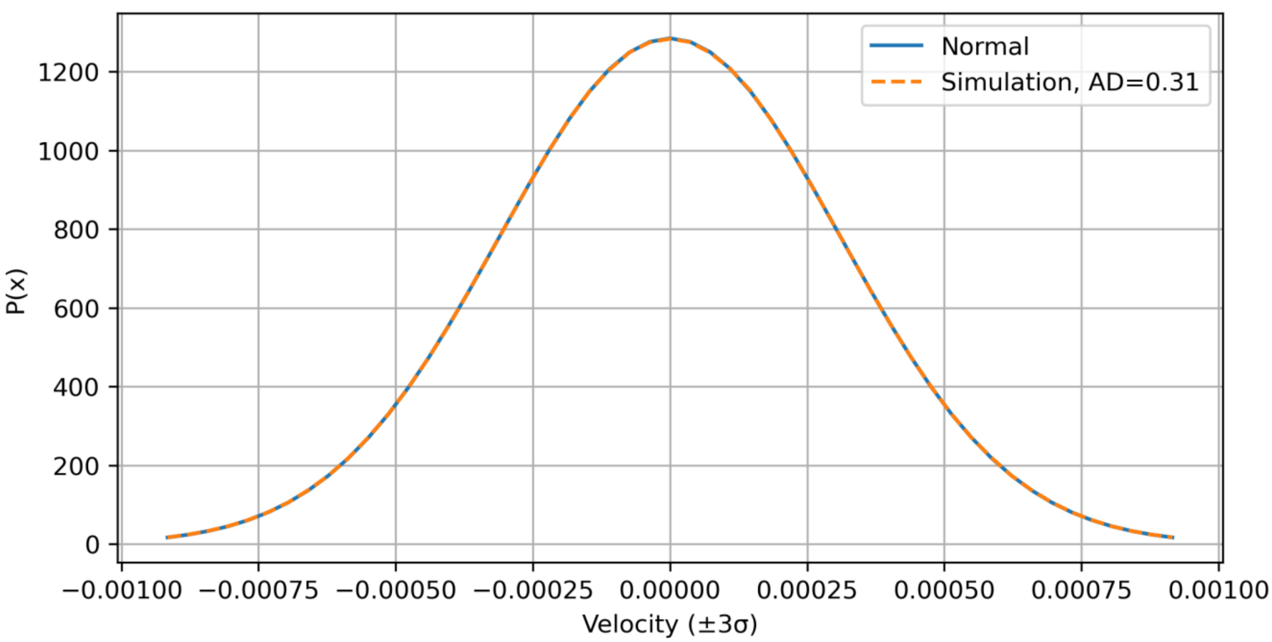

Figure SD1 Probability density function of the velocity at the horizontal x direction: Simulation data (dashed orange line) and same mean-variance normal distribution (continuous blue line, indistinguishable from the dashed line).

Density and temperature

We divided the simulation domain into 100 horizontal slabs of equal height (L/100) from bottom to top. Every 25 000 collisions, we calculated the density and temperature in each slab. After completing 1.2 billion collisions (24 000 per particle), we averaged the calculated values to generate profiles of density and temperature per height.

Figure SD2 shows the gas density vs. height, where an exponential decrease of density with height is observed (a straight line in a plot on a logarithmic density axis). A non-equilibrium boundary layer (Knudsen layer with typical thickness of a few mean free paths) forms near the bottom, where particlewall interactions distort local distributions. As seen in the view zoomed at the bottom of the simulation box (right panel), for height < 0.6×10^{-9}, the density distribution is distorted. To exclude this effect from our results, we assumed a transition height further up, at height $\approx10^{-8}$ m. All data from lower slabs were excluded and grayed out in the plot.

Figure SD3 shows the profiles of density and temperature in linear plots. The lowest slab used is at height 1.02×10^{-8} m (determined from Figure SD2 as explained), which we treat as the base level (analogous to sea level). Densities and temperatures at all other heights are expressed as percentages of this baseline. Above a certain level (0.7×10^{-7} m in Figure SD2) the temperature fluctuates irregularly, which is a statistical effect due to the small number of particles per slab. Still, below this height (where the density falls to 0.29% of the base) the temperature profile remains remarkably flat. This suggests that the temperature is independent of altitude in this regime. Beyond that, larger fluctuations would require more simulation time for robust conclusions.

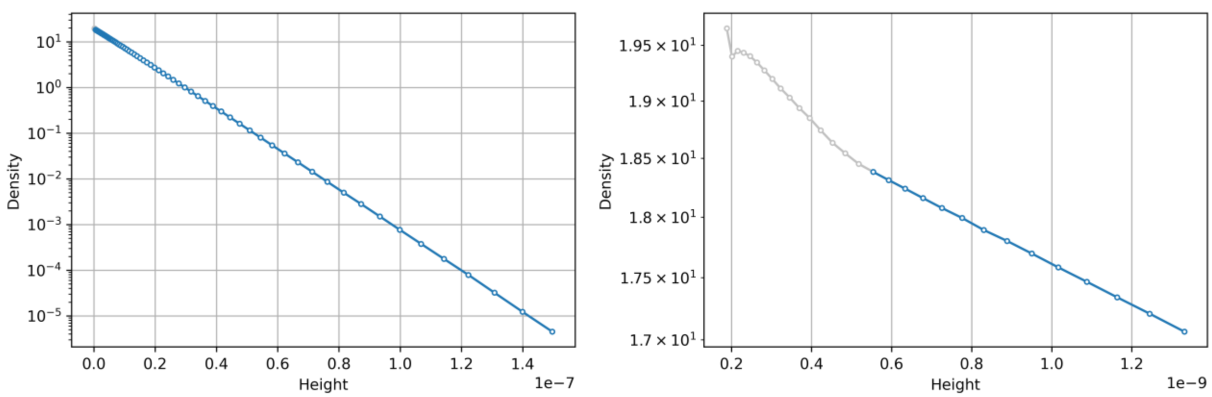

Figure SD2 Density measurements per height (logarithmic profile): (**left**) full range of scales; (**right**) zoom at the bottom of the simulation box.

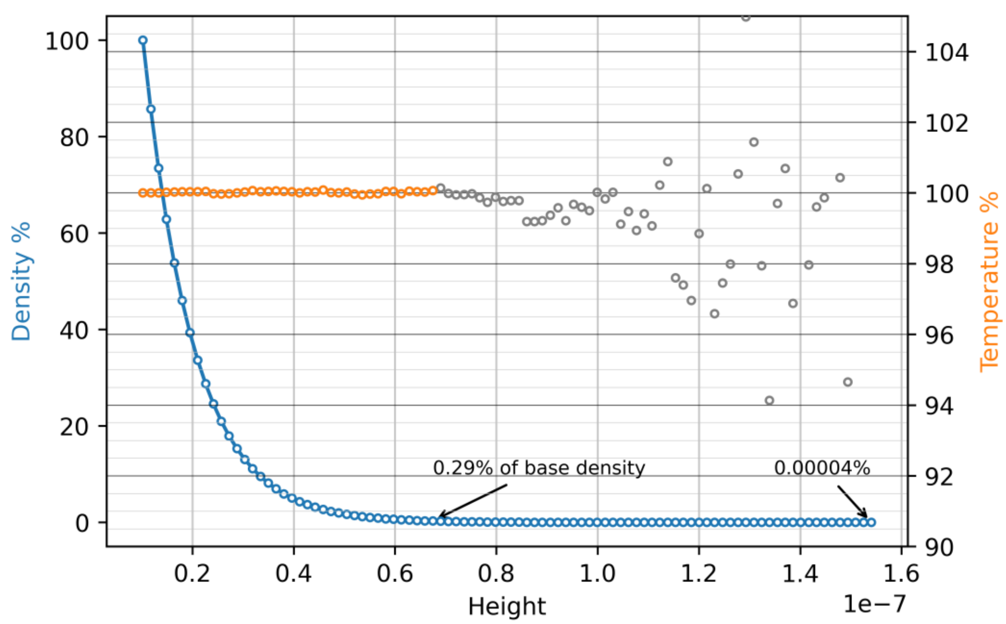

Figure SD3 Linear plots of density and temperature profiles.

To make the simulation results physically realistic, as shown in Figure 3 (in the body of the paper), we made the following conversions (rescaling). We set the base density to 1.2 kg/m³ (sea-level air density) and scale the other values accordingly using the percentages shown in Figure SD3. When the density reaches ~30% of the base, we mark it as the top of the troposphere (~10 km). The top of the stratosphere is also annotated in Figure 3. For the temperature, we set the base to 252 K and plot the profile accordingly. As seen, the temperature remains essentially constant throughout the troposphere and stratosphere. Overall, the simulation and analysis support the conclusion that, in the absence of radiation and convection, the atmosphere remains isothermal for all practical purposes.

References

Abbot, C.G., 1909. V, Note on the theory of the greenhouse. *Philosophical Magazine Series 6*, 18 (103), 32-35, doi: 10.1080/14786440708636670.

ACS (American Chemical Society), undated. *Greenhouse Gases, ACS Climate Science Toolkit*. https://web.archive.org/web/20230610031720/https://www.acs.org/climatescience/greenhousegases.html

AIP (American Institute of Physics), 2025. *The Discovery of Global Warming*. https://history.aip.org/climate/simple.htm

Arrhenius, S., 1896. XXXI. On the influence of carbonic acid in the air upon the temperature of the ground. *The London, Edinburgh, and Dublin Philosophical Magazine and Journal of Science*, 41 (251), 237-276. doi:10.1080/14786449608620846.

Arveson, P.T., 2023. Is a greenhouse heated by radiation trapping or convection blocking?. *Journal of the Washington Academy of Sciences*, 109(1), 41-62.

Ekholm, N., 1901. On the variations of the climate of the geological and historical past and their causes. *Quarterly Journal of the Royal Meteorological Society*, 27 (117), pp.1-62.

Fleming, J.R., 1998. Historical perspectives on climate change. Oxford University Press, https://books.google.gr/books?id=09RtcSCGv7gC.

Gerlich, G. and Tscheuschner, R.D., 2009. Falsification of the atmospheric CO2 greenhouse effects within the frame of physics. *International Journal of Modern Physics B*, 23 (03), 275-364.

Harde, H. and Schnell, M., 2022. Verification of the greenhouse effect in the laboratory. *Science of Climate Change*, 2 (1), 1-33, doi: 10.53234/scc202203/10.

Humphreys, W.J., 1913. Volcanic dust and other factors in the production of climatic changes, and their possible relation to ice ages. *Journal of the Franklin Institute*, 176 (2), 131-172.

IPCC (Intergovernmental Panel on Climate Change), 1990. Climate Change: The IPCC Scientific Assessment. First Assessment Report (FAR), Cambridge University Press, Cambridge, UK.

IPCC (Intergovernmental Panel on Climate Change), 2007. Climate Change 2007: The Physical Science Basis. Fourth Assessment Report (AR4), Cambridge University Press, Cambridge, UK.

IPCC (Intergovernmental Panel on Climate Change), 2021. Climate Change 2021: The Physical Science Basis. Contribution of Working Group I to the Sixth Assessment Report (AR6_ of the Intergovernmental Panel on Climate Change; Masson-Delmotte, V., Zhai, P., Pirani, A., Connors, S.L., Péan, C., Berger, S., Caud, doi: 10.1017/9781009157896.

Koutsoyiannis, D., 2014. Entropy: from thermodynamics to hydrology. *Entropy*, 16 (3), 1287–1314, doi: 10.3390/e16031287/

Nahle, N.S., 2011a. Observations on "backradiation" during nighttime and daytime. *Principia Scientific International and Biology Cabinet*, 1-16, https://principia-scientific.com/publications/New_Concise_Experiment_on_Backradiation.pdf.

Nahle, N.S., 2011b. Repeatability of professor Robert W. Wood's 1909 experiment on the theory of the greenhouse, *Biology Cabinet Online-Academic Resources and Principia Scientific International*. Monterrey, NL, USA, https://www.justproveco2.com/papers/Nahle2011GreenhouseEffect.pdf.

NOAA (National Oceanography and Atmospheric Administration), undated 1. Climate Glossary by the Climate Prediction Center of the National Weather Service, https://www.cpc.ncep.noaa.gov/products/outreach/glossary.shtml#G

NOAA (National Oceanography and Atmospheric Administration), undated 2. Weather Glossary: G's, https://www.noaa.gov/jetstream/appendix/weather-glossary-g

NOAA (National Oceanography and Atmospheric Administration), undated 3. Basics of the Carbon Cycle and the Greenhouse Effect, https://gml.noaa.gov/outreach/carbon_toolkit/basics.html

Papoulis, A., 1990. *Probability and Statistics*, Prentice-Hall, New Jersey, USA.

Pöschel, T., and Schwager, T., 2005. *Computational Granular Dynamics: Models and Algorithms*. Springer, Berlin, Heidelberg, Germany. ISBN 978-3-540-21485-4.

Poynting, J.H., 1907. LXXIV, On Prof. Lowell's method for evaluating the surface-temperatures of the planets; with an attempt to represent the effect of day and night on the temperature of the earth, *Philosophical Magazine Series 6*, 14 (84), 749-760, doi: 10.1080/14786440709463737.

Pratt, V.R., 2016. Wood's 1909 greenhouse experiment, performed more carefully, Stanford University, http://clim.stanford.edu/WoodExpt/

Schnell, M. and Harde, H., 2023. Model-experiment of the greenhouse effect. *Science of Climate Change*, 3 (5), 445-462, doi: 10.53234/scc202310/27.

Seim, T.O. and Olsen, B.T., 2020. The influence of IR absorption and backscatter radiation from CO2 on air temperature during heating in a simulated earth/atmosphere experiment. *Atmospheric and Climate Sciences*, 10, 168-185, doi: 10.4236/acs.2020.102009.

Spencer, R., 2013a. Revisiting Wood's 1909 greenhouse box experiment, Part I. Roy Spencer's Blog, https://www.drroyspencer.com/2013/08/revisiting-woods-1909-greenhouse-box-experiment-part-i/

Spencer, R., 2013b. Revisiting Wood's 1909 greenhouse box experiment, Part II. Roy Spencer's Blog, https://www.drroyspencer.com/2013/08/revisiting-woods-1909-greenhouse-box-experiment-part-ii/

Trewartha, G.T., 1954. *An Introduction to Climate*. 402 pp., McGraw-Hill, New York, https://archive.org/details/in.ernet.dli.2015.261708/.

Very, F.W., 1908. XLI, The Greenhouse theory and planetary temperatures. *Philosophical Magazine Series 6*, 16 (93), 462-480, doi: 10.1080/14786440908636529.

Wei, P.S., Chiu, H.H., Hsieh, Y.C., Yen, D.L., Lee, C., Tsai, Y.C. and Ting, T.C., 2019. Absorption coefficient of water vapor across atmospheric troposphere layer. *Heliyon*, 5(1), doi: 10.1016/j.heliyon.2019.e01145

WMO (World Meteorological Organization) 1992. International Meteorological Vocabulary; No. 182; WMO: Geneva, Switzerland, https://library.wmo.int/records/item/35809-international-meteorological-vocabulary.

Wood, R.W., 1909. XXIV, Note on the theory of the greenhouse, *Philosophical Magazine Series 6*, 17 (98), 319-320, doi: 10.1080/14786440208636602.